Available online at www.sciencedirect.com
SCIENCE DIRECT®
Journal of Solid State Chemistry 178 (2005) 3137–3144
JOURNAL OF SOLID STATE CHEMISTRY
www.elsevier.com/locate/jssc

$Ca_{6.3}Mn_3Ga_{4.4}Al_{1.3}O_{18}$—A novel complex oxide with 3D tetrahedral framework

Artem M. Abakumov[a,*], Joke Hadermann[b], Anna S. Kalyuzhnaya[a], Marina G. Rozova[a], Mikhail G. Mikheev[c], Gustaaf Van Tendeloo[b], Evgeny V. Antipov[a]

[a]*Department of Chemistry, Moscow State University, Moscow 119992, Russia*
[b]*EMAT, University of Antwerp, Groenenborgerlaan 171, B-2020 Antwerp, Belgium*
[c]*Department of Low Temperature Physics, Moscow State University, Moscow 119992, Russia*

Received 23 June 2005; received in revised form 24 July 2005; accepted 25 July 2005
Available online 25 August 2005

Abstract

A new $Ca_{6.3}Mn_3Ga_{4.4}Al_{1.3}O_{18}$ compound has been prepared by solid state reaction in a dynamic vacuum of 5×10^{-6} mbar at 1200 °C. The crystal structure of $Ca_{6.3}Mn_3Ga_{4.4}Al_{1.3}O_{18}$ was studied using X-ray powder diffraction ($a = 15.07001(5)$ Å, SG $F432$, $Z = 8$, $R_I = 0.031$, $R_P = 0.068$), electron diffraction and high resolution electron microscopy. The $Ca_{6.3}Mn_3Ga_{4.4}Al_{1.3}O_{18}$ structure can be described as a tetrahedral $[(Ga_{0.59}Mn_{0.24}Al_{0.17})_{15}O_{30}]^{18.24-}$ framework stabilized with embedded $[(Ca_{0.9}Mn_{0.1})_{14}MnO_6]^{18.24+}$ polycations, which consists of an isolated MnO_6 octahedron surrounded by a capped cube of $(Ca_{0.9}Mn_{0.1})$ atoms. The $Ca_{6.3}Mn_3Ga_{4.4}Al_{1.3}O_{18}$ structure is related to the structure of $Ca_7Zn_3Al_5O_{17.5}$, but appears to be significantly disordered due to the presence of two orientations of oxygen tetrahedra around the cationic 0,0,0 and x,x,x ($x \approx 0.17, 0.15$) positions in a random way according to the $F432$ space symmetry. The analogy between the $Ca_{6.3}Mn_3Ga_{4.4}Al_{1.3}O_{18}$ crystal structure and the structure of the "fullerenoid" $Sr_{33}Bi_{24+\delta}Al_{48}O_{141+3\delta/2}$ oxide is discussed. $Ca_{6.3}Mn_3Ga_{4.4}Al_{1.3}O_{18}$ adopts a Curie–Weiss behavior of $\chi(T)$ above $T \approx 50$ K with a Weiss temperature $\Theta = -60$ K and $\mu_{eff} = 10.57\,\mu_B$ per formula unit. At lower temperatures, the $\chi(T)$ deviates from the Curie–Weiss law indicating a strengthening of the ferromagnetic component of the exchange interaction.

Keywords: $Ca_{6.3}Mn_3Ga_{4.4}Al_{1.3}O_{18}$; Crystal structure; Electron microscopy; Magnetic properties; Fullerenoid oxide

1. Introduction

Considerable attention was recently devoted to the $A_2MnB'O_{5+\delta}$ (A = Ca, Sr, B' = Ga, Al) complex oxides with a brownmillerite-type structure due to their rich crystal chemistry, the interesting magnetic interactions between the Mn cations in mixed $+3/+4$ oxidation state and their potential application as a structural matrix for new colossal magnetoresistance materials [1–6]. In order to investigate the relationship between the crystallographic properties of such brownmillerite phases and their chemical compositions we have prepared the $Ca_2MnGa_{1-x}Al_xO_5$ solid solutions ($0.2 \leqslant x \leqslant 1.0$) [7], which exhibit a compositionally induced phase transition between the $Pnma$ ($x \leqslant 0.5$) and the $I2mb$ ($x > 0.5$) variants of the brownmillerite structure due to a change of the ordering pattern of the infinite chains of vertex sharing (Ga, Al)O_4 tetrahedra. We have found that the brownmillerite-type solid solutions become unstable when annealed under a lowered partial oxygen pressure and yield a new cubic phase as one of the decomposition products. This new compound is structurally similar to the $Ca_7Zn_3Al_5O_{17.5}$ phase [8] and to the recently discovered $Ca_7Co_3Ga_5O_{18}$ [9,10]. This article describes the preparation, chemical composition, structural studies, building principles and magnetic properties of the new $Ca_{6.3}Mn_3Ga_{4.4}Al_{1.3}O_{18}$ compound.

*Corresponding author. Fax: +7 095 939 47 88.
E-mail address: abakumov@icr.chem.msu.ru (A.M. Abakumov).

0022-4596/$ - see front matter © 2005 Elsevier Inc. All rights reserved.
doi:10.1016/j.jssc.2005.07.028

2. Experimental

The samples were prepared using a solid state reaction in a dynamic vacuum. $CaCO_3$, MnO, Ga_2O_3 and Al_2O_3 were chosen as initial materials. The amounts of the initial reagents, taken according to the required cation compositions, were mixed under acetone in an agate mortar, pressed into pellets and placed into an alumina boat. The boat was introduced into an alumina tube, with the open end connected to a vacuum pump and the sealed end placed into a furnace. The tube was evacuated up to a residual pressure of 5×10^{-4} mbar and then heated slowly to 1000 °C keeping the pressure inside the tube not higher than 10^{-3} mbar. After the pressure reached the value of 5×10^{-6} mbar the tube was heated up to 1200 °C and annealed for 40 h, then furnace cooled under pumping. The procedure was repeated twice with intermediate regrinding.

The oxidation state of Mn in the samples was determined by iodometric titration.

Phase analysis and cell parameter determination were performed using X-ray powder diffraction (XRPD) with a Huber G670 Guinier diffractometer (Cu$K\alpha$1 radiation, image plate detector) and a Philips X'pert diffractometer (Cu$K\alpha$ radiation, reflection geometry, proportional counter). X-ray powder diffraction data for crystal structure refinement were collected on a Philips X'pert diffractometer. The JANA2000 program package was used for Rietveld refinement of the crystal structure [11].

The cation composition was confirmed by EDX analysis performed on carbon-coated polycrystalline samples with a JEOL JSM 5510 scanning microscope equipped with an INCAx-sight attachment on the Ca($K\alpha$), Mn($K\alpha$), Al($K\alpha$) and Ga($L\alpha$) lines. Samples for transmission electron microscopy were made by grinding the powder sample in ethanol and depositing it on a holey carbon grid. Electron diffraction (ED) patterns were obtained using a Philips CM20 electron microscope. High resolution electron microscopy (HREM) observations were made on a JEOL 4000EX instrument. Image simulations were carried out with the MacTempas software.

The magnetization in a range 5–250 K at 0.25 T was measured by vibrating sample magnetometer PARC 155 "Princeton Applied Research".

3. Results and discussion

3.1. Synthesis and composition

The formation of the $Ca_7Zn_3Al_5O_{17.5}$-like phase was first observed during the preparation of the brownmillerite-based $Ca_2MnGa_{1-x}Al_xO_5$ solid solutions. Successive annealing of the $Ca_2MnGa_{0.8}Al_{0.2}O_5$ sample twice at 1000 °C and once at 1100 °C for 40 h in sealed evacuated silica tubes resulted in a decomposition of the brownmillerite phase formed at the first step of the preparation. Instead of the $Ca_2MnGa_{0.8}Al_{0.2}O_5$ brownmillerite, a mixture of the new phase with a face-centered cubic lattice and the $Ca_{1-x}Mn_xO$ solid solution was obtained. The iodometric titration of this two-phase mixture resulted in an oxidation state of Mn close to +2 (in contrast to $V_{Mn}=+3$ in the initial sample) that implies a reduction of the sample during several evacuation and heating cycles. An obvious similarity between the XRPD patterns of the new compound and those of $Ca_7Zn_3Al_5O_{17.5}$ [8] and recently discovered $Ca_7Co_3Ga_5O_{18}$ [9,10] allows to assume a close resemblance between these crystal structures and to propose the probable $Ca_7Mn_3(Ga,Al)_5O_{18-\delta}$ composition for the new phase in the Ca–Mn–Ga–Al–O system. This composition was verified by the syntheses of numerous samples with various cation ratios, performed under dynamic vacuum starting from the initial mixtures with $V_{Mn}=+2$. A single phase material was obtained for the $Ca_{6.3}Mn_3Ga_{4.4}Al_{1.3}O_{17.85}$ initial bulk composition. The XRPD pattern of this sample was completely indexed on a face-centered cubic lattice with $a=15.0683(1)$ Å. The iodometric titration revealed the oxidation state of Mn to be equal to +2.11(5), which corresponds to the oxygen stoichiometry O_{18} within the precision of this technique. The cation ratio Ca:Mn:Ga:Al = 43.8(9):21.5(9):26.0(13):8.8(6), as determined by EDX analysis, is in reasonable agreement with the nominal $Ca_{6.3}Mn_3Ga_{4.4}Al_{1.3}O_{18}$ (Ca:Mn:Ga:Al = 42:20:29.3:8.7) composition. Decreasing the overall content of Ga and Al in the initial mixture results in the appearance of an admixture of $Ca_{1-x}Mn_xO$ solid solutions with different Ca/Mn ratio (about 6% of $Ca_{0.6}Mn_{0.4}O$ for the $Ca_7Mn_3Ga_4AlO_{18-\delta}$ initial composition) whereas a decreasing Mn content leads to the $Ca_5Ga_6O_{14}$ admixture. Nevertheless, despite the fact that no single phase samples except the $Ca_{6.3}Mn_3Ga_{4.4}Al_{1.3}O_{18}$ one, were obtained, different values of the lattice parameter for different sample compositions and a significant disorder over the cation sublattice of the $Ca_{6.3}Mn_3Ga_{4.4}Al_{1.3}O_{18}$ structure (see below) indicate the existence of a homogeneity range for this compound. For example, an increase of the lattice parameter up to $a=15.1024(6)$ Å was observed for the $Ca_7Mn_3Ga_4AlO_{18-\delta}$ sample that is related to an increasing Ga/Al ratio in comparison with $Ca_{6.3}Mn_3Ga_{4.4}Al_{1.3}O_{18}$.

3.2. Symmetry consideration and crystal structure refinement

In order to detect possible deviations from cubic symmetry an electron diffraction investigation of $Ca_{6.3}Mn_3Ga_{4.4}Al_{1.3}O_{18}$ was undertaken. The [001], [111] and [110] electron diffraction patterns of $Ca_{6.3}Mn_3Ga_{4.4}Al_{1.3}O_{18}$

are shown in Fig. 1. The ED patterns show no violation of the cubic symmetry and can be completely indexed with a face-centered unit cell with $a \approx 15.1$ Å, in agreement with the XRPD results. No other reflection conditions except $hkl: h+k, k+l, l+h = 2n$ were observed, which leads to the $F23$, $Fm\bar{3}$, $F432$, $F\bar{4}3m$ or $Fm\bar{3}m$ space groups.

The space group for the Rietveld structure refinement was chosen from this set using the compatibility with the atomic arrangement of the $Ca_7Zn_3Al_5O_{17.5}$ crystal structure [8], which provides good starting model for the $Ca_{6.3}Mn_3Ga_{4.4}Al_{1.3}O_{18}$ crystal structure. The $Ca_7Zn_3Al_5O_{17.5}$ crystal structure is described in the space group $F23$ and comprises three independent Ca atoms at one $24f$ $(x,0,0)$ and two $16e$ (x,x,x) positions, a Zn atom at the $16e$ position and (Zn, Al) atoms at the $4a$ (0,0,0), $4b$ (1/2,1/2,1/2), $16e$ and $24g$ $(x,1/4,1/4)$ positions and oxygen atoms at the $4c$ (1/4,1/4,1/4), $16e$, $24f$ and two $48h$ (x,y,z) positions. As a first step the space group $F23$ and the atomic coordinates of the $Ca_7Zn_3Al_5O_{17.5}$ structure were tested as an initial model. After refining the occupancy factors for the cation positions, atomic coordinates and atomic displacement parameters (ADPs) the reliability factors for the $F23$ model ($R_I = 0.079$, $R_P = 0.090$) did not reach acceptable values indicating a poor agreement between the experimental and calculated diffraction profiles. The atomic coordinates x_1,x_1,x_1 and x_2,x_2,x_2 for pairs of the $16e$ positions of the same kinds of atoms in the $F23$ groups were found to follow the $x_1 \approx 1 - x_2$ relation with good precision. For example, for two Ca atoms the x values were observed to be $x_1 = 0.6101(3)$ and $x_2 = 0.3848(3)$. The atomic coordinates of two oxygen $48h$ positions correspond to each other as $x,y,z \Leftrightarrow \bar{z},y,x$. This indicates that these positions can be symmetrically equivalent and that the space symmetry of the $Ca_{6.3}Mn_3Ga_{4.4}Al_{1.3}O_{18}$ structure can be higher than $F23$. Several additional features were observed on the difference Fourier map. A positive peak at the $4d$ (3/4,3/4,3/4) position was set as an extra oxygen atom, which results in a nominal O_{18} stoichiometry. This decreases the reliability factors to $R_I = 0.074$, $R_P = 0.087$. The difference Fourier map near the $16e$ (x,x,x) $x \approx 0.17$, 0.83 cation positions shows the presence of couples of negative and positive peaks (Fig. 2) that indicates a possible splitting of these positions. This disorder cannot be adequately explained by a symmetry lowering since $F23$ is the lowest symmetry group for the F-centered cubic lattice. Splitting every $16e$ cation position into two (x,x,x) positions with close x values and twice smaller occupancy drastically improves the agreement between the experimental and calculated data ($R_I = 0.035$, $R_P = 0.069$). As a conclusion, the refinement of the structure in the $F23$ space group revealed symmetrically equivalent couples of $16e$ and $48h$ positions, possible disorder at the cation sublattice and an extra oxygen atom at the $4d$ (3/4,3/4,3/4) position.

The most symmetric $Fm\bar{3}m$ space group was also tested for the initial model of the $Ca_{6.3}Mn_3Ga_{4.4}Al_{1.3}O_{18}$ crystal structure. The atomic positions of $Ca_7Zn_3Al_5O_{17.5}$ being transformed into the $Fm\bar{3}m$ space group yield the merging of some positions of the $F23$ group into positions with a higher multiplicity: two $16e$ (x,x,x) Ca positions and two $16e$ (Zn, Al) positions into the $32f$ (x,x,x) positions, and the $4c$ and $4d$ oxygen positions into the $8c$ position of the $Fm\bar{3}m$ space group. The cation sublattice does not deviate significantly from the $Fm\bar{3}m$ symmetry, but the $F23 \rightarrow Fm\bar{3}m$ transformation introduces a significant disorder in the oxygen sublattice: two $48h$ (x,y,z) oxygen positions merge into a $192l$ one, and the $16e$ position is transformed into a $32f$ position. An occupancy factor $g = 0.5$ should be assigned to these positions. The refinement of this model results in $R_I = 0.092$, $R_P = 0.101$. The additional maxima near the cation $32f$ (x,x,x), $x \approx 0.17$ position were also observed on the difference Fourier map, as it was found in the $F23$ model. Splitting this position into two (x,x,x) positions with $x \approx 0.176$ and 0.148 with $g = 0.5$ decreases the reliability factors down to $R_I = 0.048$, $R_P = 0.081$.

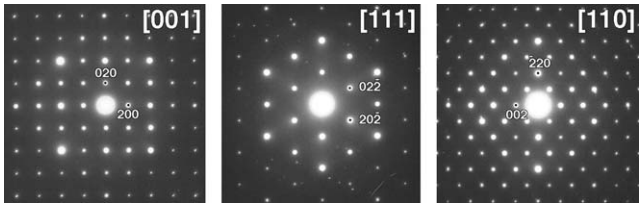

Fig. 1. [001], [111] and [110] electron diffraction patterns of $Ca_{6.3}Mn_3Ga_{4.4}Al_{1.3}O_{18}$.

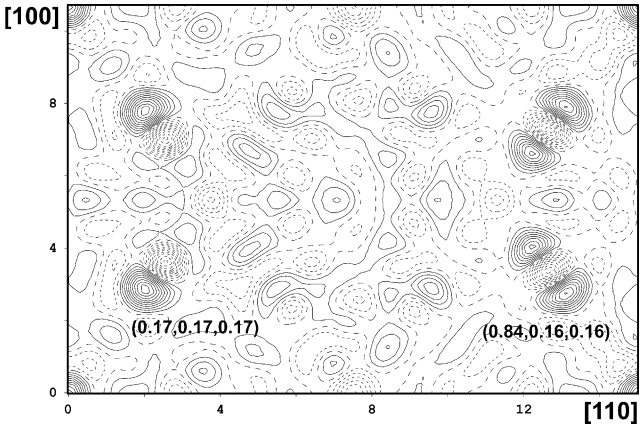

Fig. 2. (110) section of the difference Fourier map drawn near the $16e$ (x,x,x) $x \approx 0.17$, 0.83 cation positions of the $F23$ structure. Solid and dashed contours mark positive and negative peaks, respectively. Contours are drawn over every $0.2\,e^-/Å^3$.

From the preliminary refinements in the $F23$ and $Fm\bar{3}m$ space groups one can expect that the symmetry group of the $Ca_{6.3}Mn_3Ga_{4.4}Al_{1.3}O_{18}$ crystal structure is a subgroup of $Fm\bar{3}m$ and a supergroup of $F23$, i.e. $Fm\bar{3}$, $F432$, $F\bar{4}3m$. The $Fm\bar{3}$ and $F\bar{4}3m$ groups do not allow to eliminate the disorder of the (x,y,z) oxygen positions observed in the $Fm\bar{3}m$ model and can be ruled out. The best result was achieved in the $F432$ space group with the atomic positions listed in Table 2. The Ca, Mn, Ga and Al atoms cannot be unambiguously distributed among the cation sublattice, taking into account the small difference in scattering power of the Ca, Mn and Ga atoms, but a tentative distribution can be proposed based on the refined electron densities, chemical composition and interatomic distances. The electron densities were estimated as $\sim 20.5\,e^-$/atom for the Ca1 and Ca2 positions, $\sim 25.1\,e^-$/atom for the Mn position, $\sim 23.7\,e^-$/atom for the Ga1 position, $\sim 27.2\,e^-$/atom for the Ga2 position, $\sim 16.6\,e^-$/atom for the Ga3 position and $\sim 9.5\,e^-$/atom for the Ga4 position. Both Ca1 and Ca2 positions cannot be fully occupied by Ca atoms simultaneously because then there will be 7 Ca atoms per formula unit in contrast to 6.3 Ca atoms in the real composition. One can assume that the Ca2 position is partially occupied with Mn^{2+} cations since Al^{3+} and Ga^{3+} are too small to be placed in the 6-fold coordinated cavity around the Ca2 position with an average Ca2–O distance of 2.345 Å ($r(Ca^{2+}) = 1.14$ Å, $r(Mn^{2+}) = 0.96$ Å, $r(Ga^{3+}) = 0.76$ Å, $r(Al^{3+}) = 0.67$ Å for CN = 6 [12]). Thus, the 9-fold coordinated Ca1 position was assumed to be occupied by Ca atoms only, and both Ca and Mn cations were placed at the 6-fold coordinated Ca2 position. The octahedrally coordinated Mn position seems to be occupied only by Mn atoms, whereas the tetrahedrally coordinated Ga1 and Ga2 positions are filled jointly by Ga and Al according to the refined electron densities. Despite that the Ga1 position is surrounded by a cube of O4 atoms, the real coordination environment is a tetrahedron since the occupancy factor of the O4 position is equal to 0.5. The Ga3 and Ga4 positions cannot be filled simultaneously because of a short Ga3–Ga4 distance, so that the $g(Ga3) + g(Ga4) = 1$ condition should be fulfilled. The remaining Ga, Al and Mn atoms were distributed among these positions as $Ga3 = 0.168Ga + 0.45Mn$ and $Ga4 = 0.25Ga + 0.132Al$. This satisfies the refined electron densities at these positions and the compound composition $Ca_{6.3}Mn_3Ga_{4.4}Al_{1.3}O_{18}$, and agrees well with the experimentally determined Mn oxidation state of $+2.11$. The final refinement was performed with an isotropic approximation for the ADPs and with a common ADP for the oxygen atoms. The crystallographic parameters for $Ca_{6.3}Mn_3Ga_{4.4}Al_{1.3}O_{18}$ are listed in Table 1, atomic coordinates, occupancy factors and ADPs are listed in Table 2, and selected interatomic distances are shown in Table 3. The experimental, calculated and difference X-ray diffraction profiles are shown in Fig. 3.

The results of the Rietveld refinement were further confirmed by HREM observations. The [001] HREM image of $Ca_{6.3}Mn_3Ga_{4.4}Al_{1.3}O_{18}$ is shown in Fig. 4. On this image the bright dots correspond to the projection of the columns of oxygen atoms in between the cations. The best agreement between experimental and calculated image was found at a thickness of $t = 15$ Å and a defocus $\Delta f = -300$ Å.

Table 1
Crystallographic information for $Ca_{6.3}Mn_3Ga_{4.4}Al_{1.3}O_{18}$

Composition	$Ca_{6.3}Mn_3Ga_{4.4}Al_{1.3}O_{18}$
Space group	$F432$
a (Å)	15.07001(5)
V (Å^3)	3422.48(1)
Z	8
Radiation, λ (Å)	Cu$K\alpha$, 1.54184
Calculated density (g cm^{-3})	4.0635
2θ range, step, deg	9.00–115.00, 0.02
Number of reflections	151
Refinable parameters	18
R_I, R_P, R_{wP}	0.031, 0.068, 0.089

Table 2
Atomic coordinates and displacement parameters for $Ca_{6.3}Mn_3Ga_{4.4}Al_{1.3}O_{18}$

Atom	Site	Occupancy	x/a	y/b	z/c	U_{is} (Å^2)
Ca1	24e	1	0.2104(1)	0	0	0.0134(9)
Ca2	32f	0.825Ca/0.175Mn	0.38892(8)	x	x	0.0072(7)
Mn	4b	1	1/2	1/2	1/2	0.003(1)
Ga1	4a	0.66Ga/0.34Al	0	0	0	0.011(1)
Ga2	24d	0.80Ga/0.20Al	0	1/4	1/4	0.0092(5)
Ga3	32f	0.168Ga/0.45Mn	0.1746(1)	x	x	0.0029(8)
Ga4	32f	0.25Ga/0.132Al	0.1472(2)	x	x	0.013(2)
O1	96j	1	0.2453(3)	0.1458(2)	0.0686(3)	0.005(1)
O2	8c	1	1/4	1/4	1/4	0.005(1)
O3	24e	1	0.3684(4)	0	0	0.005(1)
O4	32f	0.5	0.0703(4)	x	x	0.005(1)

Table 3
Most relevant interatomic distances (Å) for $Ca_{6.3}Mn_3Ga_{4.4}Al_{1.3}O_{18}$

Ca(1)–O(1)	2.485(4) × 4	Ga1–O4	1.835(7) × 8
Ca1–O3	2.381(7) × 1		
Ca1–O4	2.589(7) × 4	Ga2–O1	1.881(4) × 4
Ca2–O1	2.317(5) × 3	Ga3–O1	1.969(4) × 3
Ca2–O3	2.388(2) × 3	Ga3–O2	1.967(2) × 1
Mn–O3	1.983(7) × 6	Ga4–O1	1.895(5) × 3
		Ga4–O4	2.006(7) × 1
		Ga4–O2	2.684(3) × 1

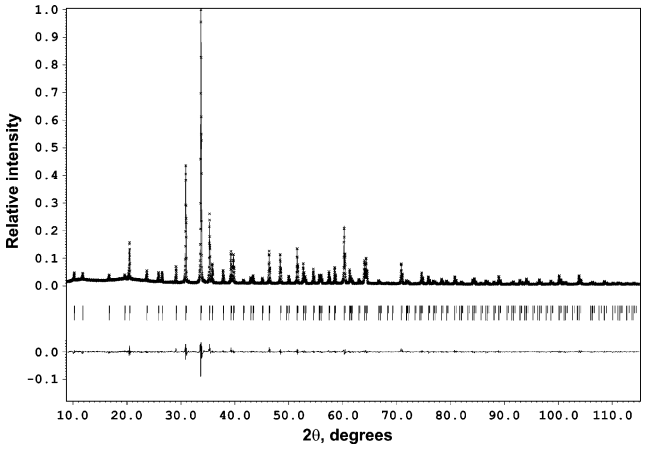

Fig. 3. The experimental, calculated and difference X-ray diffraction profiles for $Ca_{6.3}Mn_3Ga_{4.4}Al_{1.3}O_{18}$.

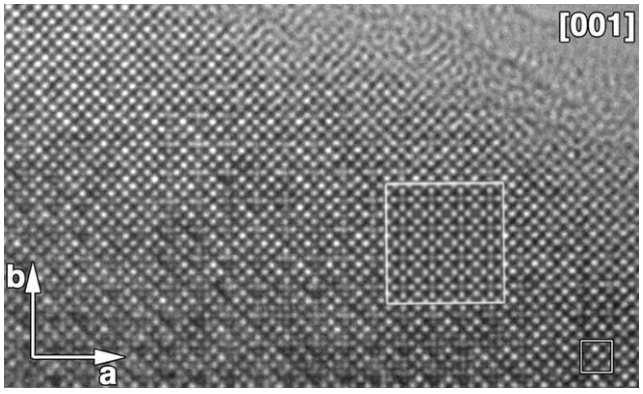

Fig. 4. [001] HREM image of $Ca_{6.3}Mn_3Ga_{4.4}Al_{1.3}O_{18}$. Calculated image ($t = 15$ Å, $\Delta f = -300$ Å) is superimposed on the experimental image.

3.3. Structural considerations

The topology of the $Ca_{6.3}Mn_3Ga_{4.4}Al_{1.3}O_{18}$ structure can be understood if one considers combinations of partially filled cationic and anionic positions which can be simultaneously present in the structure without abnormally short interatomic distances. This analysis was performed by transforming the refined $F432$ structure into the $F23$ subgroup. Such transformation affects the atomic positions resulting in the following set of coordination environments: Ga1 is tetrahedrally coordinated either by 4 $O4_1$ atoms or by 4 $O4_2$ atoms (subscript indexes denote independent positions of the $F23$ group derived from the x,y,z (1) and $y,x,\bar{z}$ (2) symmetry operation sets of the $F432$ group). Ga2 is located in tetrahedra formed by two $O1_1$ and two $O1_2$ atoms. Ga3 and Ga4 positions produce pairs of simultaneously present atoms $Ga3_1$–$Ga4_2$, $Ga3_2$–$Ga4_1$ and $Ga3_1$–$Ga3_2$. These atoms are also tetrahedrally coordinated ($Ga3_1$: $O1_1 \times 3$, $O2_1 \times 1$; $Ga3_2$: $O1_2 \times 3$, $O2_2 \times 1$; $Ga4_1$: $O1_1 \times 3$, $O4_1 \times 1$; $Ga4_2$: $O1_2 \times 3$, $O4_2 \times 1$) and form a framework together with the Ga1 and Ga2 atoms. Two configurations of the framework are possible, which are produced by the x,y,z and $y,x,\bar{z}$ symmetry operation sets of the $F432$ group and can be transformed into each other by a rotation over 90° around the ⟨001⟩ axes (Fig. 5). Ga3 and Ga4 atoms with the surrounding oxygen atoms form tetrahedral clusters shown in Fig. 6, top. In the Ga3 cluster four tetrahedra have one common corner (O2 atom) positioned at the center of the cluster. Contrarily, in the Ga4 cluster the tetrahedra have no common corners, and the vertices formed by the O4 atoms point outward of the center of the cluster. Such clusters are present in the $Ca_7Zn_3Al_5O_{17.5}$ structure, where they are located in an ordered manner, corresponding to one of the framework configurations shown in Fig. 5. However, the $Ca_{6.3}Mn_3Ga_{4.4}Al_{1.3}O_{18}$ structure has more oxygen atoms than the $Ca_7Zn_3Al_5O_{17.5}$ one. These extra O2 atoms are located at the centers of the Ga4 clusters, according to full occupancy of the O2 position. This atomic arrangement should be more thoroughly discussed. Being placed at the special (1/4,1/4,1/4) (Fig. 6, top right) position, this O2 atom is separated by a rather large distance of 2.68 Å from the neighboring Ga4 cations and is underbonded. Indeed, even if we consider that the O2 atom in the Ga4 cluster is surrounded by 4 Ga cations, the bond valence sum (BVS) can be estimated as −0.308, and this is far away from the nominal value of −2. On the other hand, the O2 atoms forming a common vertex of four Ga3 tetrahedra in the Ga3 cluster appear to be overbonded: BVS of −2.50 and −2.12 was obtained for this atom being surrounded by either four Mn^{2+} or four Ga^{3+} cations, respectively. This consideration leads to the conclusion that an occurence of the idealised Ga3 and Ga4 clusters, as they are shown in Fig. 6, top, is not possible in the $Ca_{6.3}Mn_3Ga_{4.4}Al_{1.3}O_{18}$ structure. Instead of being separated into two different clusters, the Ga3 and Ga4 tetrahedra should form mixed clusters. Most probably, such mixed clusters should comprise three Ga3 and one Ga4 tetrahedron (Fig. 6 bottom) since such arrangement allows to achieve reasonable BVS values

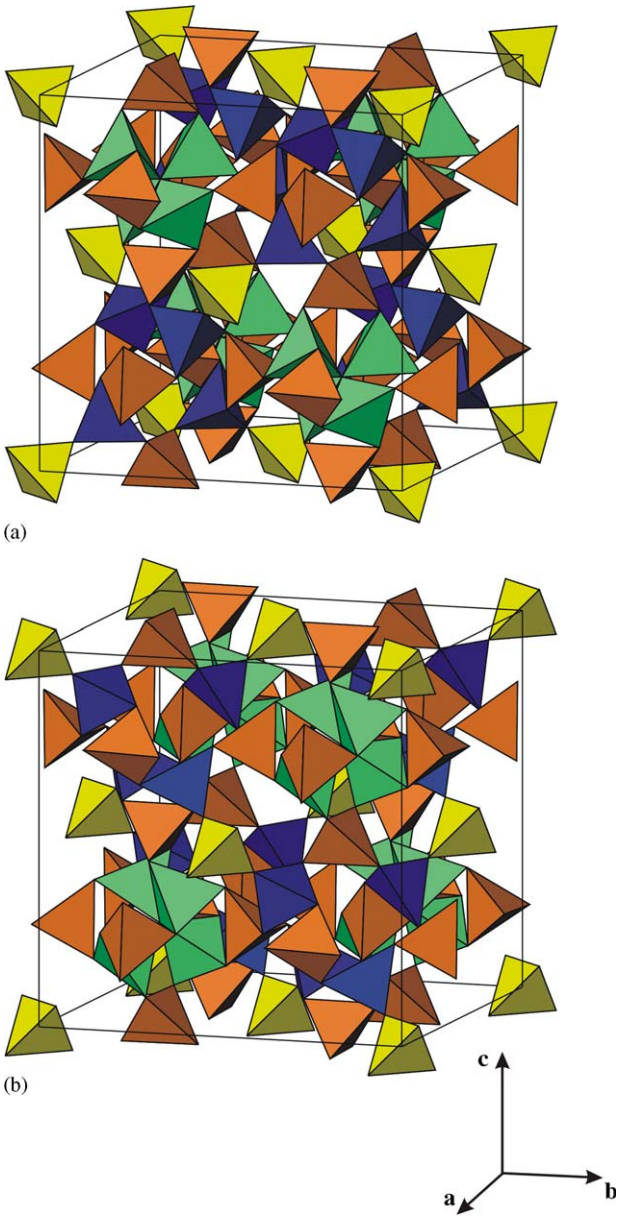

Fig. 5. Two configurations of the idealized tetrahedral framework in the $Ca_{6.3}Mn_3Ga_{4.4}Al_{1.3}O_{18}$ structure, which are produced by the x,y,z (a) and $y,x,\bar{z}$ (b) symmetry operation sets of the $F432$ group. Ga1, Ga2, Ga3 and Ga4 are located at the yellow, brown, green and blue tetrahedra, respectively. Ca1, Ca2, Mn and O3 atoms are omitted for clarity.

for the O2 atoms. For example, if the O2 atom is surrounded by three Mn^{2+} at 1.969 Å and one Ga^{3+} at 2.684 Å, a BVS value of −1.952 is obtained. The combination of two Mn^{2+} at the Ga3 position and two Ga^{3+} at the Ga4 position leads already to a much lower BVS value of −1.40. The proposed arrangement accounts for the larger occupancy factor of the Ga3 position in comparison with that of the Ga4 one. Grins et al. proposed a similar explanation for the disorder in the $Ca_7Co_3Ga_5O_{18}$ structure [10].

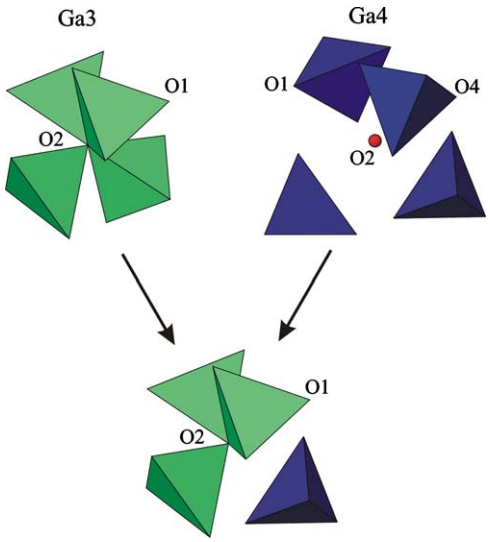

Fig. 6. Top: the idealized Ga3 and Ga4 tetrahedral clusters. Bottom: a formation of mixed Ga3–Ga4 cluster in the $Ca_{6.3}Mn_3Ga_{4.4}Al_{1.3}O_{18}$ structure. Ga3 and Ga4 atoms are located at the centers of green and blue tetrahedra, respectively.

The O3 atoms do not participate in the tetrahedral framework and form octahedra around the Mn atoms. The Mn–O3 octahedra together with the Ca1 and Ca2 atoms fill the cages in the tetrahedral framework (Fig. 7a). The MnO_6 octahedra are isolated from each other and from the tetrahedral framework. The $Ca_{6.3}Mn_3Ga_{4.4}Al_{1.3}O_{18}$ compound exhibits an onion-skin-like structure where the Mn atom, chosen as a central point, is surrounded by the enclosed O_6, $(Ca,Mn)_{14}$ and $(Ga, Al, Mn)_{42}O_{104}$ shells (Fig. 7b). From this point of view, the $Ca_{6.3}Mn_3Ga_{4.4}Al_{1.3}O_{18}$ compound demonstrates a certain similarity to the structural organization of the "fullerenoid" $Sr_{33}Bi_{24+\delta}Al_{48}O_{141+3\delta/2}$ oxide [13], where the onion-skin-like structure is also present, and the largest sphere in this structure has a geometry virtually identical to that of D2d isomer of the C_{84} fullerene. However, the analogy with fullerene is based on pure geometrical resemblance since the bonding in complex oxides is essentially more ionic than that in carbon materials. The tetrahedral framework of the $Ca_{6.3}Mn_3Ga_{4.4}Al_{1.3}O_{18} = (Ca_{0.9}Mn_{0.1})_{14}Mn(Ga_{0.59}Mn_{0.24}Al_{0.17})_{15}O_{36}$ structure can be described as a 3D $[(Ga_{0.59}Mn_{0.24}Al_{0.17})_{15}O_{30}]^{18.24-}$ polyanion stabilized with the embedded $[(Ca_{0.9}Mn_{0.1})_{14}MnO_6]^{18.24+}$ polycations.

3.4. Magnetic properties

The temperature dependence of the magnetic susceptibility $\chi(=M/H)$ is shown in Fig. 8. At high temperatures χ vs. T obeys the Curie–Weiss law with a Weiss temperature $\Theta\sim -60$ K and an effective moment $\mu_{eff} = 10.57\,\mu_B$ per formula unit. The last value is close to the theoretical estimate of $10.08\,\mu_B$ calculated in the

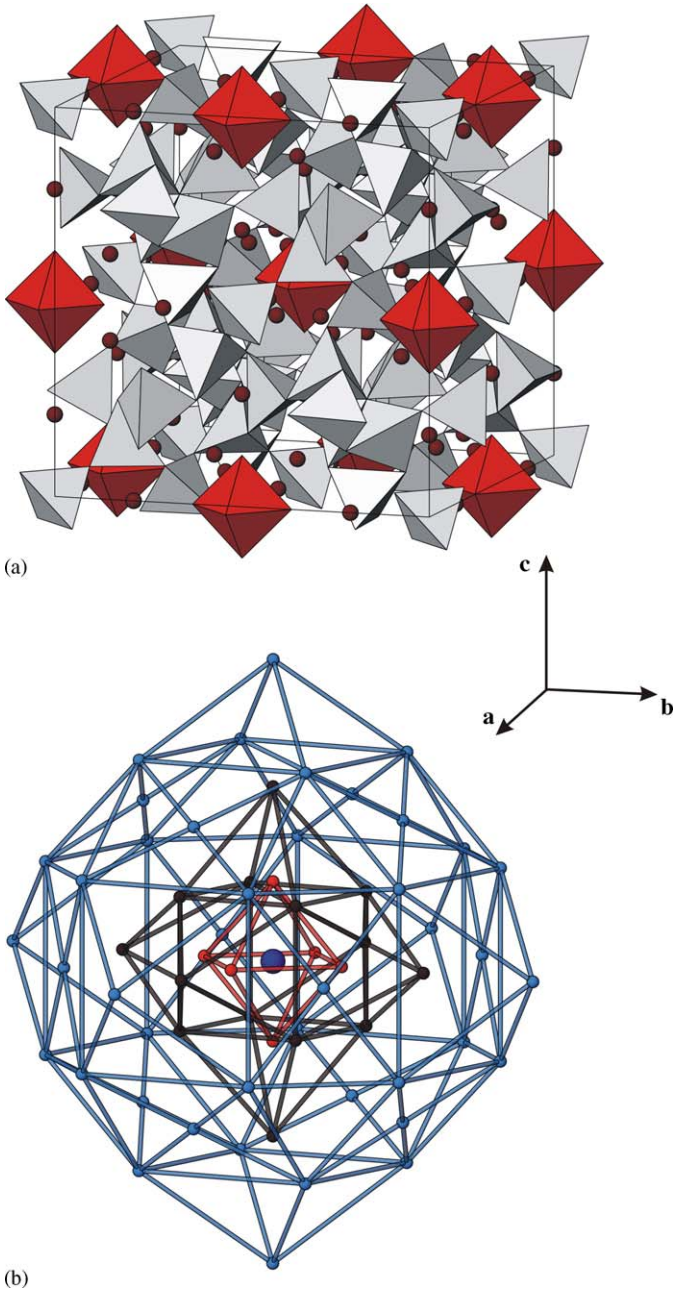

Fig. 7. Top: positions of the MnO_6 octahedra (red), Ca1 and Ca2 atoms (brown spheres) in the unit cell. The *F*23 ordered structure is shown for simplicity. Bottom: onion-skin-like structure with the Mn atoms located as a central point (blue sphere) surrounded by the enclosed O_6 (red), $(Ca,Mn)_{14}$ (brown) and $(Ga, Al, Mn)_{42}O_{104}$ (light blue) shells.

assumption of *g*-factor $g = 2$. In accordance with the chemical composition $Ca_{6.3}Mn_3Ga_{4.4}Al_{1.3}O_{18}$ there are approximately 90% of Mn^{2+} ($S = 5/2$) and 10% of Mn^{3+} ($S = 2$). The negative Weiss temperature indicates a dominance of the antiferromagnetic exchange interactions in this diluted magnetic system. At low temperatures, the χ vs. T dependence deviates from the Curie–Weiss law indicating a strengthening of the ferromagnetic component of the exchange interaction. This strengthening can be tentatively attributed to the presence of Mn ions in different valence states which opens a way to ferromagnetic double exchange interaction.

4. Conclusions

A new $Ca_{6.3}Mn_3Ga_{4.4}Al_{1.3}O_{18}$ compound was discovered in the Ca–Mn–Al–Ga–O system as a product of the reduction of the $Ca_2MnGa_{0.8}Al_{0.2}O_5$ brownmillerite and then prepared as a single phase material. The structure consists of a tetrahedral [$(Ga_{0.59}Mn_{0.24}$

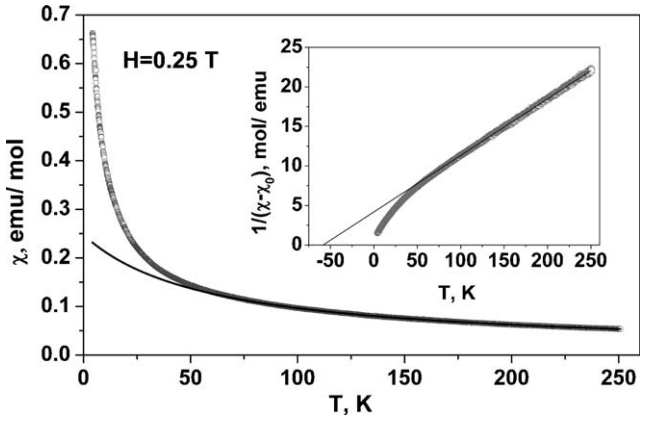

Fig. 8. Temperature dependence of magnetic susceptibility $\chi(=M/H)$ of $Ca_{6.3}Mn_3Ga_{4.4}Al_{1.3}O_{18}$. The solid line represents fit in accordance with the Curie–Weiss law. The inset shows the inverse magnetic susceptibility, where χ_0 represents temperature independent contribution.

$Al_{0.17})_{15}O_{30}]^{18.24-}$ framework stabilized with the embedded $[(Ca_{0.9}Mn_{0.1})_{14}MnO_6]^{18.24+}$ polycations. A high degree of disorder in the structure can be attributed to the random orientation of the tetrahedra around the Ga3 and Ga4 atoms in order to achieve proper bonding conditions for the O2 atoms placed at the centers of the tetrahedral clusters. The joint occupation of the tetrahedrally coordinated positions in the framework by Ga and Al is not a necessary condition for the stability of this structure type. We already succeeded in the preparation of the Al-free compound with approximate $Ca_7Mn_{2.3}Ga_{5.7}O_{18-y}$ composition and $a = 15.1220(8)$ Å. This indicates a large ability of this structure type in adapting to changes in the chemical composition.

Acknowledgments

The work was supported in part by the IAP V-1 program of the Belgium government and the RFBR project 04-03-32785-a. AMA is grateful to the INTAS for the Fellowships grant for Young Scientists YSF-05-55-1035 and to Russian Science Support Foundation for the financial support.

References

[1] A.M. Abakumov, M.G. Rozova, B.Ph. Pavlyuk, M.V. Lobanov, E.V. Antipov, O.I. Lebedev, G. Van Tendeloo, D.V. Sheptyakov, A.M. Balagurov, F. Bouree, J. Solid State Chem. 158 (2001) 100–111.
[2] A.M. Abakumov, M.G. Rozova, B.Ph. Pavlyuk, M.V. Lobanov, E.V. Antipov, O.I. Lebedev, G. Van Tendeloo, O.L. Ignatchik, E.A. Ovtchenkov, Yu.A. Koksharov, A.N. Vasi'ev, J. Solid State Chem. 160 (2001) 353–361.
[3] A.J. Wright, H.M. Palmer, P.A. Anderson, C. Greaves, J. Mater. Chem. 11 (2001) 1324–1326.
[4] A.J. Wright, H.M. Palmer, P.A. Anderson, C. Greaves, J. Mater. Chem. 12 (2002) 978–982.
[5] P.D. Battle, A.M. Bell, S.J. Blundell, A.I. Coldea, D.J. Gallon, F.L. Pratt, M.J. Rosseinsky, C.A. Steer, J. Solid State Chem. 167 (2002) 188–195.
[6] V.Yu. Pomyakushin, A.M. Balagurov, T.V. Elzhov, D.V. Sheptyakov, P. Fisher, D.I. Khomskii, V.Yu. Yushankhai, A.M. Abakumov, M.G. Rozova, E.V. Antipov, M.V. Lobanov, S.J.L. Billinge, Phys. Rev. B 66 (2002) 184412.
[7] A.M. Abakumov, A.S. Kalyuzhnaya, M.G. Rozova, E.V. Antipov, J. Hadermann, G. Van Tendeloo, Solid State Sci. 7 (2005) 801–811.
[8] V.D. Barbanyagre, T.I. Timoshenko, A.M. Il'inets, V.M. Shamshurov, Powder Diffract. 12 (1997) 22–26.
[9] S.Ya. Istomin, E.V. Antipov, G. Svensson, J.P. Attfield, V.L. Kozhevnikov, I.A. Leonidov, M.V. Patrakeev, E.B. Mitberg, J. Solid State Chem. 167 (2002) 196–202.
[10] J. Grins, S.Ya. Istomin, G. Svensson, J.P. Attfield, E.V. Antipov, J. Solid State Chem. 178 (2005) 2197–2204.
[11] V. Petricek, M. Dusek, JANA2000: Programs for Modulated and Composite Crystals, Institute of Physics, Praha, Czech Republic, 2000.
[12] R.D. Shannon, Acta Crystallogr. A 32 (1976) 751–767.
[13] M. Hervieu, B. Mellene, R. Retoux, S. Boudin, B. Raveau, Nat. Mater. 3 (2004) 269–274.